Very Long Baseline Interferometry and the VLBA
ASP Conference Series, Vol. 82, 1995
J. A. Zensus, P. J. Diamond, and P. J. Napier (eds.)

Printed June 13, 1995

CHAPTER 8

What the VLBA Can Do for You: Capabilities, Sensitivity, Resolution, and Image Quality

R. C. WALKER

NATIONAL RADIO ASTRONOMY OBSERVATORY

Abstract This chapter gives a basic description of what can be done with the VLBA. First the types of observations for which the array was built are reviewed. The special characteristics of the array that facilitate such observations are described. Then the major factors that determine whether a particular experiment can be done are discussed in some detail. These factors are the resolution, (u, v) coverage, sensitivity, and image quality.

Contents

8.1 Basic Capabilities of the VLBA

The VLBA was designed primarily as an imaging instrument. It is capable of making high quality images of radio astronomical sources with a resolution of about 1 milliarcsecond (mas). Such resolution allows morphological studies to be made of objects of solar system size throughout our galaxy and of parsec scale throughout the observable universe. To allow detection by an instrument of such high resolution, an object must emit a large amount of radiation from a small region so the primary targets of the VLBA will be very energetic. Likely targets include active galactic nuclei, extragalactic supernovae, active stars, pulsars, and astrophysical masers.

Compact, highly energetic objects often show structural changes on time scales of hours to years on size scales that can be resolved with the VLBA. This gives the instrument the capability of making astrophysically interesting "movies" that can be compared with models of the evolution of radio sources. This is in contrast with most of astronomy where the structural evolution of objects can only be deduced by finding different objects at different stages of such evolution.

In addition to imaging, the VLBA was designed to be able to make highly accurate geometric measurements. It will be able to measure the absolute positions of compact radio sources with an accuracy of under a mas and the relative positions of pairs of sources to perhaps tens of microarcseconds. To place this in context, objects in the Galaxy move roughly 6 mas yr^{-1} year relative to background radio sources because of galactic rotation and they have parallaxes greater than about 0.1 mas (1 mas for an object at a distance of 1 kpc). Accurate position measurements can be used to measure distances through parallax, to measure proper motions, and to relate observations made at a variety of wavelengths. Also, significant tests of relativity using gravitational bending by solar system objects can be made.

The accurate geometry measurements also allow studies to be made of the dynamics of the earth. The relative positions of the antennas of the array can be determined with an accuracy of about a centimeter now and perhaps as good as a millimeter in the future. Plate tectonic motions are of the order of several centimeters per year and are routinely measured by VLBI arrays including VLBA antennas. It is somewhat sobering to consider that the catalog of positions of the VLBA antennas, with their massive concrete foundations buried deep in the ground, will have to include velocities. Position errors of only a few cm will adversely affect a number of types of observations on the VLBA and the Hawaii antenna is expected to be moving at about 9 cm yr^{-1} relative to the rest of the array. The geometric measurements can also be used to determine earth orientation parameters such as the position of the rotation axis on the sky (precession and nutation), the position of the rotation axis on the earth's crust (polar motion), and the rotation rate of the earth. Such measurements provide information about the dynamics of the earth from the core to the atmosphere.

Perhaps one of the most important goals of the VLBA is to make it possible for astronomers who are not experts in VLBI to make VLBI observations. The effort involved in calibrating VLBI data will be greatly simplified. Software for VLBI will be provided in environments widely familiar to the astronomical community (AIPS at present). Documentation (including these proceedings) and assistance are provided to guide inexperienced users. The VLA has been a success in making first rate radio observations available to the astronomical community at large. It is intended that the VLBA will do for VLBI what the VLA did for centimeter-wave linked interferometry.

8.1.1 Special Capabilities for Imaging

Many of the fundamental characteristics of the VLBA were set by the need to make images. The number of antennas (10) and their diameters (25 m) were a compromise that would give good (u,v) coverage, adequate sensitivity, and fit within a budget that stood a chance of being funded. The locations of the antennas were chosen for optimum (u,v) coverage under the geographical constraints that they must be on land and on United States territory (for cost and operational simplicity). A two-dimensional array was selected so that it would have reasonable (u,v) coverage for equatorial and southern declination sources. The astrophysics that can be derived from observations can vary with frequency. Therefore a wide range of receivers was installed on the VLBA antennas and it is possible to switch between them rapidly. Especially good antennas were built so that observations at 43 GHz are possible now and at 86 GHz will be possible in the future. All receivers provide dual polarization so it is possible to do polarimetry.

Most types of VLBA science depend on good calibration. The VLBA has very stable receivers and good pointing. All electronics and cables were designed for phase stability and to avoid problems that could cause closure errors. For amplitude calibration, the VLBA system provides for continuous measurement of system noise through synchronous detection of a low-level, switched noise calibration signal. This is far superior to the once-per-scan measurements typical of past VLBI. A pulse-calibration (also called phase-calibration or "phase-cal") system, along with a round trip system that monitors the electrical length of the cable carrying the LO reference signal from the maser to the receivers, is provided to measure any delay and phase shifts in the electronics. This allows all separate channels to be aligned in phase and allows all data times to be referenced to the maser. The possibility that this system may also provide superior amplitude calibration is being studied.

The 25 meter antennas of the VLBA are smaller than many of those previously used for VLBI so special care has to be taken to compensate for their inherent sensitivity limitations. A high-gain, shaped design was used that has an efficiency of about 70% compared to the 50% more typical of large antennas. Low-noise receivers, with typical system temperatures of near 30 K at the intermediate frequencies, are used. A wide-band recording system is available for all observations, even those on strong sources. The recording system has modes which can be used in special cases that give 2 or 4 times the normal bit rate. Highly stable clock and LO systems, along with a well known geometry, provide the maximum possible coherence times allowed by the atmosphere. High, dry sites were chosen where possible for the antennas. Finally, provisions were made to use the VLBA with other antennas, many of which have much greater sensitivity. The array configuration is centered on the VLA which, when used as a phased array, is equivalent to a 115 m antenna. The correlator can handle up to 20 antennas in one pass.

A promising technique for imaging complex sources is multi-frequency synthesis (MFS; see chapter 16). This technique is based on using observations over a range of frequencies to fill in the (u, v) coverage. To use this technique, receivers must have wide bandwidths—10% or more is desired—and the electronics must be able to utilize frequencies spread over the full front end bandwidth either simultaneously or with rapid switching. The VLBA receivers all have adequate bandwidth for this technique and some, especially the 20 cm and 2 cm receivers, have bandwidths of 25 to 35 %. Up to eight distinct baseband frequencies can be observed simultaneously within a 500 MHz IF bandwidth and switching between different IF bands can be done in a few seconds.

The amount by which a (u, v) track is broadened by using a range of frequencies is a function of the (u, v) value itself. The widening is by a percentage of the (u, v) value that is equal to the percentage of observing frequency that is spanned. This means that there is much less broadening of the tracks near the center of the (u, v) plane than in the outer regions. The VLBA was designed with a centrally condensed (u, v) coverage for which the tracks near the center are much more densely packed than in the outer regions. This allows the MFS observing style to fill in the (u, v) plane over a very wide range of (u, v) spacings.

Several capabilities of the VLBA are provided to enhance spectral line observations. The correlator is able to provide large numbers of spectral points, up to 1024 per baseband channel. It is able to provide significant numbers of points in full polarization modes. It also provides the autocorrelation spectra which can be of great value for spectral line calibration. For sensitivity, spectral line observations are unable to take advantage of the wide bandwidths available since the signals being observed are fundamentally of limited bandwidth. The VLBA system provides both 4-level sampling and oversampling to improve the SNR in cases that are not bit rate limited. Between these capabilities and some more subtle properties of the correlator to be discussed later, the VLBA system will be nearly twice as sensitive as previous VLBI systems for spectral line observations.

It will be very important for sensitivity on the VLBA to make it able to use phase connection for calibration. This is the procedure in which a nearby calibrator is used to calibrate the interferometer phases. It is the standard calibration technique for linked interferometers such as the VLA. Without phase connection, the VLBA will be limited to observing sources that can be detected to each antenna within a coherence time. With it, sources can be observed that can just be detected using all the data on all baselines for the full time of an experiment. The difference in detection levels is nearly two orders of magnitude (see chapter 17).

A number of properties of the VLBA should enhance the chances that phase connection will work and will become a normal mode of observing. The geometry of the array will be very well known from geodetic type observations. A highly accurate a priori geometry model, obtained from the geodetic community, will be used on the correlator. The fast moving antennas and quick synchronization capabilities of the correlator allow for short scans and rapid switching between calibrator and program source. The dual-frequency, 4/13 cm system and the geodetic GPS receivers at the sites will aid in ionospheric calibration. The fast-slewing and low-elevation capabilities of the antennas will help solve for the atmosphere if necessary. A large calibrator list is being assembled so that there should be a known reference source within a few degrees of any target.

8.1.2 Special Capabilities for Geodesy and Astrometry

The VLBA is an extremely capable tool for geodesy and, especially, astrometry. Compared to most of the antennas used for geodesy, the VLBA antennas are very sensitive. This allows the use of short scans and allows observation of weak sources. The antennas slew relatively rapidly ($90°$ min^{-1} in azimuth, $30°$ min^{-1} in elevation) and can reach very low elevations ($2.25°$). This allows the rapid observations of many sources all over the sky, including at elevations where the troposphere is the dominant term, that are needed to solve for the tropospheric delay. This is important since tropospheric fluctuations are the dominant source of errors in geodetic and astrometric observations. The VLBA is outfitted with dual-frequency 4/13 cm receiving systems which allow calibration of the ionosphere and which are compatible with other geodetic VLBI systems throughout the world. The 4 cm system can take both IFs from the same polarization (RCP) with different LO signals in order to obtain an instantaneous spanned bandwidth of over a gigahertz. A phase-cal system and a round trip LO cable length measuring system are provided so that all delays can be referred back to the maser.

The VLBA only has 8 baseband converters (BBCs) and therefore can only observe 8 different frequencies simultaneously. This is significantly fewer than the 14 video converters available in the Mark III system. For the bandwidth synthesis observing style used for geodesy (see chapter 18), this will probably be adequate but just barely. It will be adequate mainly because the individual channels can have up to 16 MHz bandwidths and the single-band delays can be used to constrain the multi-band delay. There is also a rapid frequency switching capability which can be used if necessary.

Other geodetic instruments will continue to be needed because the VLBA covers only a limited fraction of the earth's surface and because it will have limited availability for geodesy. Measurements of tectonic-plate motions require antennas on other plates besides the two or three covered by the VLBA. Careful monitoring of earth orientation requires very frequent observations. In fact some of the most active VLBI sites in the world prior to the VLBA were ones like the

NASA site near Fairbanks, Alaska, which most astronomers probably barely know exists. It will also be useful to include other antennas with the VLBA to improve longitude coverage. With any non-global array, the edge antennas have a region of sky that cannot be observed because of lack of mutual visibility with any other antenna in the array. This makes calibration of the troposphere at those antennas more difficult. If the array includes antennas all around the earth, this can be avoided.

8.1.3 Operational Advantages of the VLBA

The VLBA is a single instrument under one management with facilities for all phases of a VLBI observation from proposal handling through observing, correlating, and post-processing. It has 10 identical antennas with a common maintenance system and good feedback from the correlator. It has a large staff all with responsibility to make the whole thing work. The correlator is large enough to handle all observations rapidly. All of this may sound like it should not make a large difference compared to the collections of separate observatories used for previous VLBI, but experience suggests that it may well be as important any other capabilities of the array. In fact, by setting a standard for comparison in VLBI performance, the VLBA has already raised the quality of VLBI observations from observatories around the world.

One significant capability of a unified array is the ability to respond quickly to targets of opportunity. If a nova, supernova, or other short lived event occurs, the VLBA can be observing in a matter of hours or even minutes. There is also a concept of dynamic scheduling where observing projects can be shuffled to allow the more demanding ones to take advantage of good weather or to minimize the impact of equipment failures or seriously bad weather.

8.2 Frequency Coverage

The antennas used for VLBI are only sensitive to certain frequencies. The antennas themselves impose limitations on the lowest and highest frequencies that can be observed. At the low end, the wavelengths become too long for the optics in normal parabolic antennas. At the high end, the surface accuracy and the pointing limit performance. Special designs that can reach extreme high or low frequencies eventually run into problems with the earth's atmosphere. The ionosphere cuts off any incoming radiation below a few megahertz. Various absorption lines in the troposphere make observations difficult at many frequencies in the millimeter and shorter wavelength region. At centimeter wavelengths, the troposphere and ionosphere, while not totally benign, are limited problems. Also it is reasonably easy to build large, sensitive antennas for use in this region. Historically, most VLBI has been done in the range 327 MHz to 22 GHz with significant recent effort between 43 and 300 GHz.

Within the range set by the antennas and atmosphere, the possible observing frequencies are determined by the specific receivers available on each antenna. Efforts have been made to coordinate the receivers available on many antennas throughout the world. The standard observing frequencies currently used by the global network (consisting mostly of the European VLBI Network (EVN) and the VLBA) are 327, 609, 1420, 1664, 2268, 4992, 8418, 22230, and 43200 MHz (see chapter 20).

Table 8.1 gives detailed information on the more extensive set of frequencies available on the VLBA. Each band has a separate receiver and feed and is labeled using the VLBA band naming conventions based on the wavelength. The approximate frequency range for each band, as determined by observations, is given in the second column. The third column gives the percentage bandwidth spanned which is of interest for MFS and bandwidth synthesis observations. The fourth and fifth columns give the best and the typical zenith SEFDs currently available on the VLBA antennas. The SEFD, or *system equivalent flux density*, is the ratio of the system temperature and the gain and is a good overall measure of system sensitivity. It is described further in section 8.4.1 below. It is likely that, as various problems with the initial installations are corrected, the average SEFDs will be lowered to values near the current best. The sixth and seventh columns give the rms noise levels for VLBA data on a single baseline in two minutes and in an image based on eight hours of data from all ten antennas. Both of these noise levels assume the typical SEFD, a recorded bit rate of 128 Mbps, and a "correlator" efficiency (see sensitivity discussion below) of 0.5 which is probably lower than the actually value. The final column gives the maximum resolution in mas that can be obtained with the VLBA at that band.

Not all frequencies within each receiver band are good for observing because of radio frequency interference (RFI). In a few cases, the RFI is so strong that special filters have been installed at certain sites. Also efforts have been made to work with the owners of the offending transmitters to minimize the impact on the VLBA systems. With time, the VLBA staff will try to characterize the RFI environment at each station as an aid in choosing optimum observing frequencies. In most bands, there is a range of frequencies that is protected for astronomy by international agreements and the recommended observing frequencies will usually include that range. However, at the lower frequencies where RFI is worst, the protected ranges do not have adequate bandwidth for typical continuum observations. Observers will usually be forced to take their chances with unprotected frequencies.

For spectral line observations, it is of course necessary to observe at the frequency of the line. Most VLBI spectral line observations are of masers which have adequate brightness for detection, although some studies of non-masing molecules seen in absorption against compact background sources have been made. For reference, the known astrophysical maser lines below about 100 GHz are listed in table 8.2 on page 141.

Table 8.1: VLBA frequency coverage, sensitivity, and resolution

Band (cm)	Frequency Range[(a)] (GHz)	Fract. Bandw. (%)	Best Zenith SEFD (Jy)	Typical Zenith SEFD (Jy)	Baseline Noise $\Delta S^{128,2m}$ (mJy)	Image Noise $\Delta I_m^{128,8h}$ (μJy/bm)	Max. Res. (mas)
90	0.312–0.345[b]	10	2000	2200	35	340	22
50	0.600–0.630[c]	5 (< 1)	1900	2200	35	340	12
20	1.30–1.85[d]	35	280	310	5.0	48	5
13	2.13–2.35	9	270	350	5.6	54	3
13[e]	2.13–2.35	9	360	440	7.1	68	3
6	4.50–5.14	13	240	300	4.8	47	1.4
4	7.88–8.93	12	240	340	5.5	53	0.9
4[e]	7.88–8.93	12	320	430	6.9	67	0.9
2	12.0–15.4[f]	25	400	530	8.6	82	0.5
1	21.1–24.6	15	700	990	16	150	0.3
7mm	39.5–45.5	14	830	1320	21	200	0.17

Notes: [a] Range over which SEFD was below 1.4 times nominal in measurements on the first 4 antennas. [b] RFI may restrict range. [c] RFI filter normally restricts range to 609–613 MHz. [d] Because of RFI, FD and KP are filtered below 1350 MHz and SC has a 700–1000 MHz IF filter. Above 1700 MHz there is considerable RFI. [e] With 13/4 cm dichroic and focus optimized for 4 cm. [f] Design specification.

8.2.1 Frequency Resolution

The frequency resolution of a VLBA or other VLBI observation is set by the observing baseband channel bandwidth and by the number of spectral points provided by the correlator. For the VLBA, baseband bandwidths between 62.5 kHz and 16 MHz, in factor of 2 steps, are available. The correlator is inherently a spectral line correlator and can provide a maximum 2048 spectral points per baseline with up to 1024 in each baseband channel. See chapters 2 and 7 for more details. Lesser numbers of channels can be provided by doing some combination of smaller FFTs and by averaging spectral points on-line. The observer will need to specify the desired correlator mode based on the desired frequency resolution for spectral line observations or on the expected delay uncertainties for continuum observations.

8.3 (u, v) Coverage and Resolution

For high quality imaging, it is desirable to have the best possible coverage of the (u, v) plane, which is effectively the telescope aperture. As a reminder, each baseline between a pair of antennas provides a point in the (u, v) plane which is determined by the observing frequency and by the projected separation of the antennas as seen from the source. As the earth rotates, the projection changes so

Table 8.2: Astrophysical maser frequencies

Molecule	Formula	Frequency (MHz)	VLBA Receiver
Hydroxyl	OH	1612.231	20 cm
Hydroxyl	OH	1665.402	20 cm
Hydroxyl	OH	1667.359	20 cm
Hydroxyl	OH	1720.530	20 cm
Hydroxyl	OH	4660.42	6 cm
Hydroxyl	OH	4765.562	6 cm
Hydroxyl	OH	6030.747	future
Hydroxyl	OH	6035.092	future
Methanol	CH3OH	6668.518	future
Hydroxyl	OH	7761.747	4 cm
Hydroxyl	OH	7820.125	4 cm
Hydroxyl	OH	8135.870	4 cm
Hydroxyl	OH	8189.587	4 cm
Methanol	CH3OH	12178.595	2 cm
Hydroxyl	OH	13441.417	2 cm
Ammonia	NH3	18499.393	
Methanol	CH3O H	19967.3961	
Water	H2O	22235.08	1 cm
Methanol	CH3OH	23121.0242	1 cm
Methanol	CH3OH	25124.87	1 cm
Silicon monoxide	SiO	42519.3	7 mm
Silicon monoxide	SiO	42820.54	7 mm
Silicon monoxide	SiO	43122.03	7 mm
Methanol	CH3OH	44069.43	7mm
Silicon monoxide	SiO	86243.35	planned
Silicon monoxide	SiO	86846.89	planned
Methanol	CH3OH	97980.97	

the baseline sweeps out a track (part of an ellipse) in the (u, v) plane. The (u, v) coverage of an array is the combination of the (u, v) tracks from all baselines provided by the array. It shows where the array samples the Fourier transform of the source image (see chapter 1).

The (u, v) coverage determines several important capabilities of an array. The maximum extent of the coverage determines the resolution. The synthesized beam size will be approximately the ratio of the observing wavelength to the maximum baseline length. The actual value will depend on details of the data weights, the (u, v) coverage, and the parameters used in the imaging programs. Since the resolution depends on the baseline lengths in wavelengths, (u, v) coverages are normally displayed in such units. The ability of an array to see large features depends on the coverage of short baselines. If short spacings are missing, the image will show only high spatial frequency structures which may be only the lumps and bumps on some large scale, relatively smooth structure and the image can be quite deceptive. Finally, the ability to image complex sources with interferometer array data depends on measuring a large number of points in the (u, v) plane and on not leaving large regions of the (u, v) plane unsampled. A perfect image can only be made if all points in the (u, v) plane (in other words, in the image transform) are measured, which is never the case. The deconvolution process used in any modern interferometer imaging can be thought of as a scheme for interpolating or extrapolating from the measured (u, v) points to all other points in (u, v) plane. Large holes in the coverage increase the difficulty of doing the interpolation correctly and uniquely. The ideal interferometer array covers a very wide range of baselines and provides (u, v) coverage that is as uniform as possible.

It is not entirely obvious how to quantify the complexity of a source that can be imaged with an interferometer. If the coverage is reasonably uniform, a rule of thumb that works fairly well for full (u, v) tracks at high declinations is that the area of the source, measured in synthesized beam areas, should be smaller than about the square of the number of baselines (Readhead and Wilkinson 1978). This can be understood if you consider a (u, v) grid with a cell size of about the spacing between (u, v) tracks in the radial direction, the smallest cell size for which most cells could be sampled. The number of such cells that would be sampled along any radius is about equal to the number of baselines. Therefore the total number of sampled cells in the two-dimensional grid is about the number of baselines squared. This can then be thought of as the number of independent measurements from which one will solve for the flux density at some number of points on the sky, each independent point being about the size of the beam. Since the number of unknowns cannot exceed, but can equal, the number of measurements, this sets the limit on the number of beam areas on the sky that can contain emission and still be imaged.

The (u, v) coverage for the VLBA for sources at four different declinations is shown in figure 8.1 on the facing page. The scale for the plots is in thousands of kilometers and would need to be divided by the observing wavelength to get

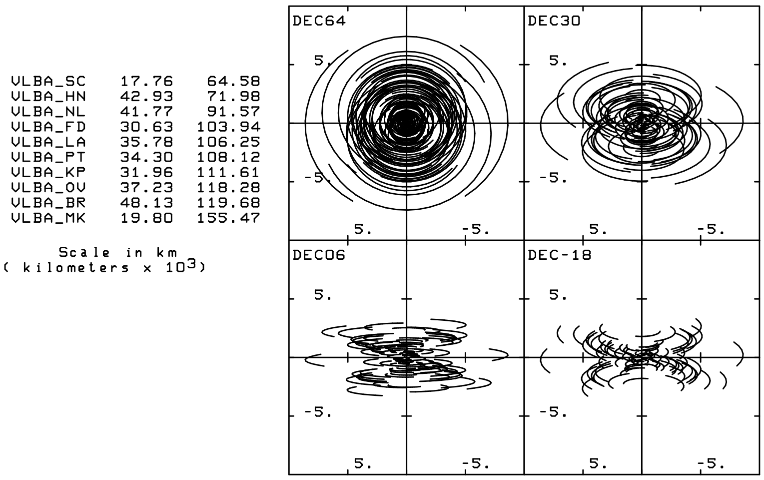

Figure 8.1: VLBA (u, v) coverage.

the usual (u, v) plot scale. The locations of the VLBA antennas were chosen to optimize the coverage consistent with constraints imposed by geography and by the requirement that all antennas be on United States territory. With ten antennas, a number set by a compromise between the (u, v) coverage, the size (sensitivity) of each antenna, and cost, it is difficult to both cover a wide range of spacings and to obtain uniform coverage of the (u, v) plane. The selected configuration is a compromise between these goals. The coverage of the very longest spacings is somewhat sparse, but it is those spacings that can be filled in well in joint observations with other VLBI observatories, especially the EVN (see chapter 20).

The coverage with a global array consisting of the VLBA and the 7 core stations of the EVN (not including the stations in China) is shown in figure 8.2. Adding the European stations, which between themselves have no baselines longer than 2000 km, dramatically improves the (u, v) coverage on long spacings at high declinations.

If a source contains structures with a wide range of scales, it is important to observe with a wide range of spacings. The minimum baseline on the VLBA is 236 km in length and the coverage for structures requiring baselines less than about 500 km will be marginal with pure VLBA data. Proper imaging of such sources will require using more than just the VLBA. A global network observation has a few more short baselines, but not a lot more. MERLIN (Thomasson 1986; Wilkinson 1991) provides good coverage below about 200 km and combining VLBI and MERLIN data should prove very productive. However there is still relatively poor coverage from about 200 to 500 km. The (u, v) coverage on these scales, showing the contribution from the EVN and MERLIN to VLBA data, is shown in figure 8.3. NRAO has long term plans to add 4 antennas to the

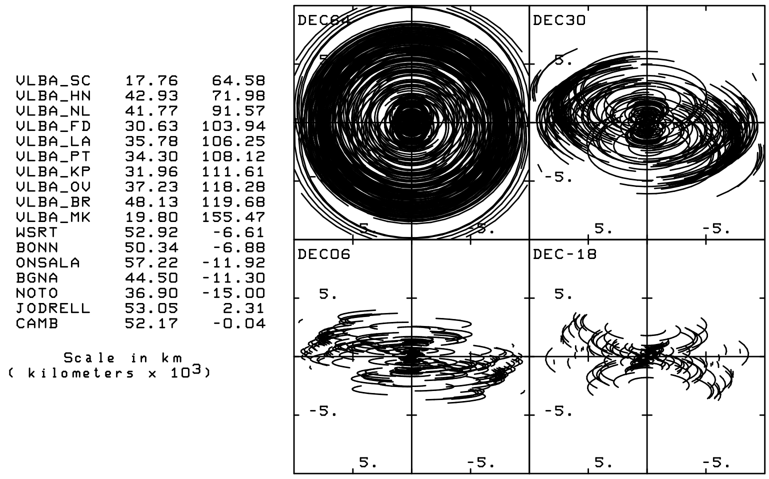

Figure 8.2: Global network (u, v) coverage. VLBA plus 7 core stations of the EVN.

VLA/VLBA to cover this range (in addition to a South American antenna for improved north-south coverage on long baselines).

Table 8.1 gives the maximum resolution available with the VLBA at each observing band. The resolution with the global array will be about 20 % higher which is close to the limit set by the size of the earth for ground-based observations. The maximum size of a smooth feature that can be imaged with an interferometer array is set by the shortest baselines available. A rule of thumb is that features larger than the fringe spacing on a baseline twice as long as the shortest in the array cannot be imaged well. For the VLBA, the shortest baseline is 36 times shorter than the longest so features up to about 18 times the resolution can be imaged. Note that there is no problem imaging compact features separated by more than this amount.

Another interesting plot for planning purposes is shown in figure 8.4. This shows the regions in frequency/resolution space that are covered by a wide variety of radio astronomical instruments ranging from VLBI to single antennas. This might help in understanding how observations made at a variety of instruments and frequencies relate. Note that the resolution of any instrument is a linear function of frequency and lies along a sloped line in this plot. Many scientific questions are best answered by observing at many frequencies with the same resolution. This requires observations along a vertical line in the plot and is likely to require observations with several different instruments.

VLBA_SC	17.76	64.58
VLBA_HN	42.93	71.98
VLBA_NL	41.77	91.57
VLBA_FD	30.63	103.94
VLBA_LA	35.78	106.25
VLBA_PT	34.30	108.12
VLBA_KP	31.96	111.61
VLBA_OV	37.23	118.28
VLBA_BR	48.13	119.68
VLBA_MK	19.80	155.47
AN9	34.24	107.63
AW9	33.97	107.81
AE9	34.00	107.41
WSRT	52.92	-6.61
BONN	50.34	-6.88
ONSALA	57.22	-11.92
BGNA	44.50	-11.30
NOTO	36.90	-15.00
JODRELL	53.05	2.31
CAMB	52.17	-0.04
DEFFORD	52.10	2.14

Scale in km
(kilometers x 10^2)

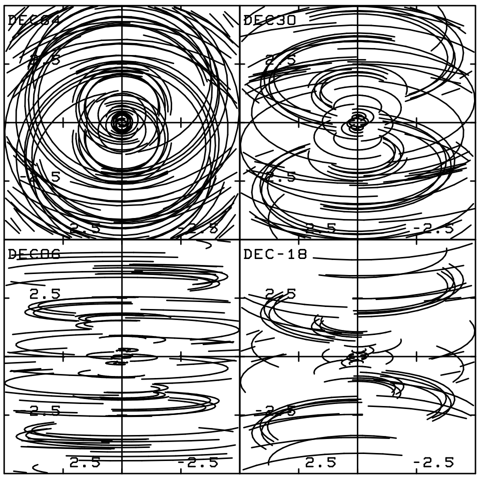

Figure 8.3: The (u, v) coverage for baselines up to 500 km using the VLBA, three VLA antennas at the ends of the arrays arms, the seven core EVN stations plus one MERLIN antenna that is not normally used with the EVN.

8.4 Sensitivity

A major factor in determining what can be observed with VLBI is sensitivity. There are two primary sensitivity limits of significance to VLBI. For VLBI observations that do not use phase referencing, the source must be detected on each baseline, or at least on the combined baselines to each station, within a coherence time. The coherence time with good electronics and well known geometry will be set by the atmosphere. It can range from a few tens of seconds at the lowest and highest frequencies to over half an hour in good weather at intermediate frequencies. To determine the sensitivity limits under these circumstances, the noise in measurements on a single baseline must be known. The other sensitivity limit of interest is noise in an image made from data from all baselines and for the full time of an observation. This determines the weakest features that can be observed near a strong source and determines the source detection limits when phase referencing can be done.

8.4.1 System Temperature and Antenna Temperature

Radio astronomers find it convenient to refer to the power of various signals from a radio telescope in terms of the equivalent temperature of a matched termination on the input of the receiver. Using the Rayleigh-Jeans approximation to the Planck black-body radiation law, such a power is given by:

$$P = kT\Delta\nu\,. \tag{8.1}$$

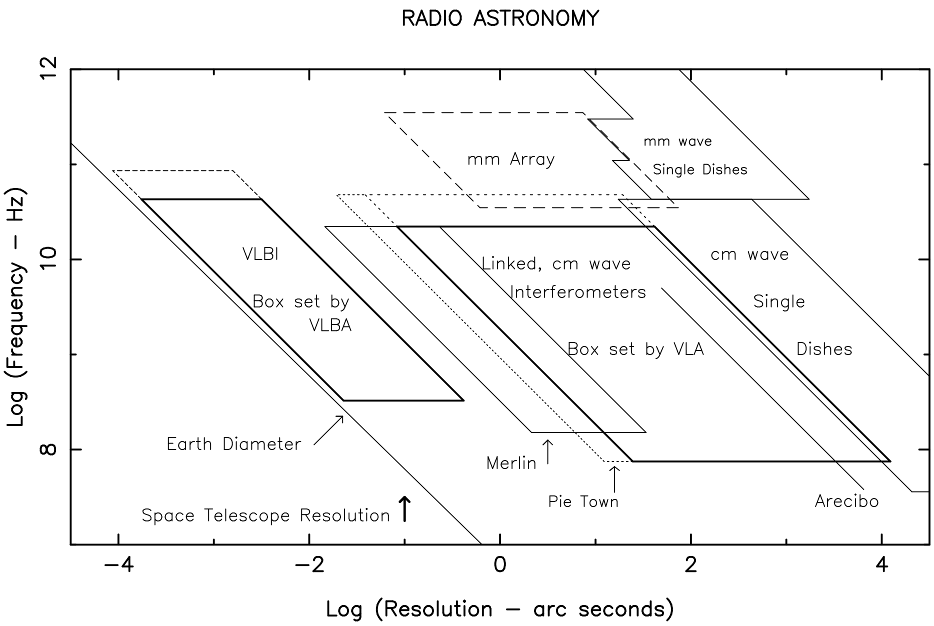

Figure 8.4: Diagram showing the frequency and resolution coverage of a variety of radio astronomy instruments. For the interferometers, the low resolution limit was set by the fringe spacing of twice the shortest spacing.

where k is Boltzmann's constant (1.38×10^{-23} joule K^{-1}) and $\Delta\nu$ is the observing bandwidth in hertz.

The power entering the feed is amplified by a factor g^2 where g is the voltage gain. Thus the powers reaching the correlator from a source and from system noise are given by:

$$P_a = g^2 k T_a \Delta\nu\,, \tag{8.2}$$

and

$$P_N = g^2 k T_s \Delta\nu\,, \tag{8.3}$$

where T_a is the *antenna temperature* for the source and T_s is the *system temperature*. T_s includes contributions from the receiver noise, feed losses, spillover, atmospheric emission, galactic background and cosmic background. The power from the source can be related to the flux density, S, the area of the antenna, A, and the antenna efficiency η using:

$$P_a = g^2 \eta A S \Delta\nu/2 = g^2 k K S \Delta\nu\,, \tag{8.4}$$

where $K = \frac{\eta A}{2k}$. From equations 8.2 and 8.4, it can be seen that K is simply the gain of the antenna in degrees K of antenna temperature per Jansky of flux density. The factor of 2 is the result of the fact that a single channel receiver only receives half of the total radiation from an unpolarized source.

It is often instructive to express the system temperature in terms of the flux density of a source that would deliver the same amount of power (SEFD = T_S/K). This is the system equivalent flux density (SEFD) mentioned earlier. Since it takes into account the efficiency, the collecting area, and the system noise, it is a useful overall measure of system sensitivity. It also has the nice property that it can be measured easily by determining the fractional increase in power obtained when pointing on and off a source of known flux density. Measurements of both the system temperature and the gain are uncertain because they both depend on the system calibration, usually a reference noise source (T_c). The system calibration cancels out for the SEFD. Values of SEFD obtained in real VLBI observations vary a great deal. Arecibo has values near 5 Jy or less at its better frequencies. Typical values on the VLBA at cm wavelengths are 250 to 500 Jy. Values of over 2000 are not uncommon at the smaller antennas with poorer receivers, or even at better antennas at non-optimal frequencies.

8.4.2 Sensitivity of a Single-Baseline Interferometer

First, consider the sensitivity of a single baseline interferometer with a single real output consisting of the product of the voltages from each of two antennas. For a complex correlator, the results of this analysis will apply separately to each channel. This calculation is commonly made using the autocorrelation function of the product (Crane and Napier 1989). Here an alternate derivation based on the rms variation of a large number of samples of a gaussian random variable will be used. This section is taken almost directly from the author's discussion of the same topic in Walker (1989).

The voltage from antenna i before sampling is the sum of voltages s_i from the source and n_i from noise. The power from antenna i is given by a constant a, which includes the gain, times the expectation value of the square of the voltage,

$$\begin{aligned} \langle P_i \rangle &= a_i \left\langle (s_i + n_i)^2 \right\rangle \\ &= a_i \left[\langle s_i^2 \rangle + \langle n_i^2 \rangle \right] \\ &= g_i^2 k (T_{ai} + T_{si}) \Delta\nu \\ &= g_i^2 k (K_i S_T + T_{si}) \Delta\nu \,. \end{aligned} \tag{8.5}$$

The expectation value of the cross term is zero—the voltages from the source and from noise are not correlated. Note that it is the total flux density seen by the antenna, S_T, that counts. For simplicity, assume that S_T is the same for all antennas, although this may not be true for very large sources that are resolved by the primary beams of the larger antennas.

The power after the cross multiplication in the correlator can be obtained in a similar way:

$$\begin{aligned}\langle P_{ij}\rangle &= \frac{\sqrt{a_i a_j}}{\eta_s}\Big\langle (s_i+n_i)(s_j+n_j)\Big\rangle \\ &= \frac{\sqrt{a_i a_j}}{\eta_s}\langle s_i s_j\rangle \\ &= \frac{g_i g_j}{\eta_s}\sqrt{K_i K_j}\,k\Delta\nu S_c\,,\end{aligned} \tag{8.6}$$

since only the signal voltages are correlated. The efficiency factor, η_s, accounts for various losses in the electronics and digital equipment. These losses are discussed in detail below. This time, the flux density that counts is the correlated flux density S_c which may be less than the total flux density, S_T.

To obtain the signal-to-noise ratio (SNR), we need to know the rms fluctuations of the correlator output. The approach that will be taken here to derive this quantity is to consider the rms fluctuations of the product of the antenna voltages for each sample. Then, the rms of the output is presumed to be reduced by the square root of the number of independent samples. A square bandpass of width $\Delta\nu$ and integration for time Δt are assumed so that the number of independent samples, by the Nyquist theorem, is $2\Delta\nu\Delta t$. The fact that the square of the rms fluctuation of a gaussian random variable (in this case, the product from the correlator) is equal to the expectation value of the variable squared minus the square of the mean is used.

$$\sigma^2(P_{ij}) = \frac{a_i a_j}{\eta_s^2}\left\langle \Big[(s_i+n_i)(s_j+n_j)\Big]^2\right\rangle - \frac{g_i^2 g_j^2}{\eta_s^2}K_i K_j k^2 S_c^2 \Delta\nu^2\,. \tag{8.7}$$

This can be rewritten, using a relation for expanding the expectation value of a product of four variables into combinations of expectation values of products of two variables (Davenport and Root 1958; see also footnote and references in Thompson, Moran and Swenson 1986, p. 156), to obtain,

$$\begin{aligned}\sigma^2(P_{ij}) &= \frac{a_i a_j}{\eta_s^2}\left[2\Big\langle (s_i+n_i)(s_j+n_j)\Big\rangle^2 + \Big\langle (s_i+n_i)^2\Big\rangle\Big\langle (s_j+n_j)^2\Big\rangle\right] \\ &\quad - \frac{g_i^2 g_j^2}{\eta_s^2}K_i K_j k^2\Delta\nu^2 S_c^2 \\ &= 2\frac{g_i^2 g_j^2}{\eta_s^2}K_i K_j (k\Delta\nu S_T)^2 + \frac{g_i^2 g_j^2}{\eta_s^2}(k\Delta\nu)^2(K_i S_T + T_{si})(K_j S_T + T_{sj}) \\ &\quad - \frac{g_i^2 g_j^2}{\eta_s^2}K_i K_j k^2\Delta\nu^2 S_c^2 \\ &= k^2\Delta\nu^2\frac{g_i^2 g_j^2}{\eta_s^2}\Big(K_i K_j S_c^2 + K_i K_j S_T^2 + K_i S_T T_{si} + K_j S_T T_{si} + T_{si}T_{sj}\Big)\,.\end{aligned} \tag{8.8}$$

Now to write the noise level in terms of Jy, take the square root and divide by the product of $g_i g_j\sqrt{K_i K_j}\,k\Delta\nu$ (the conversion factor from source flux to cross correlated power from equation 8.7) and $\sqrt{2\Delta\nu\Delta t}$ (for the standard deviation of the mean),

$$\Delta S_{ij} = \frac{1}{\eta_s\sqrt{2\Delta\nu\Delta t}}\sqrt{S_c^2 + S_T^2 + S_T\left(\frac{T_{si}}{K_i} + \frac{T_{sj}}{K_j}\right) + \frac{T_{si}T_{sj}}{K_iK_j}}, \tag{8.9}$$

which is the same result that is obtained using the autocorrelation of the cross product (Crane and Napier 1989; Thompson, Moran and Swenson 1986).

The above result can be generalized to non-square bandpasses by considering equation 8.9 to apply to an infinitesimally small bandpass, over which the square bandpass assumption is a good approximation. If $g_i(\nu)$ is the voltage gain as a function of frequency for antenna i, the overall bandpass used to set the Nyquist sample interval is $\int_0^\infty g_i(\nu)g_j(\nu)d\nu$. If the gains are carried through the above analysis, ΔS_{ij} becomes:

$$\Delta S_{ij} = \frac{\sqrt{\int_0^\infty g_i^2(\nu)g_j^2(\nu)\left[S_c^2 + S_T^2 + S_T\left(\frac{T_{si}}{K_i} + \frac{T_{sj}}{K_j}\right) + \frac{T_{si}T_{sj}}{K_iK_j}\right]d\nu}}{\eta_s\sqrt{2\Delta t\int_0^\infty g_i(\nu)g_j(\nu)\,d\nu}}. \tag{8.10}$$

Note that the noise of the correlated signal, S_c, and of the source power as it adds to the total powers at each antenna, S_T, both contribute to the total noise of the correlated output.

In most circumstances of interest, the source only contributes a small fraction of the total noise and the terms involving flux density can be ignored (Arecibo observers beware!). Returning to the assumption of square bandpasses:

$$\Delta S_{ij} = \frac{1}{\eta_s}\sqrt{\frac{T_{si}T_{sj}}{2\,\Delta t\,\Delta\nu\,K_i\,K_j}}, \tag{8.11}$$

or, in terms of the SEFDs:

$$\Delta S_{ij} = \frac{1}{\eta_s}\sqrt{\frac{SEFD_i \times SEFD_j}{2\,\Delta t\,\Delta\nu}}. \tag{8.12}$$

The common assumption of equal sensitivities and system temperatures it not made because that assumption, while often reasonable for the VLBA, is rarely correct for network observations.

8.4.3 Instrumental Losses

The above calculations include an observing and correlation efficiency factor η_s to account for losses that occur in any real interferometer. Depending on the details of how the correlator functions, and on the observing mode, η_s can be anywhere from about 0.9 to about 0.5. Some of the sources of such losses are:

1. Quantization losses. Most VLBI recording systems are digital in nature and record either one or two bits per sample (two or four levels per sample). Usually the samples are recorded at the Nyquist rate ($1/2\Delta\nu$), although in narrow band applications, faster sampling can be used. The losses for three useful cases available on the VLBA are: Nyquist sampling with one bit: 0.637, Nyquist sampling with two bits: 0.881, twice Nyquist sampling with two bits: 0.94. For continuum observations, the SNR is typically limited by the available recording bit rate. Therefore twice the bandwidth can be used in 1 bit mode as in 2-bit mode. If the 2-bit case losses are divided by $\sqrt{2}$ to account for the reduced bandwidth, the comparable loss is 0.623 which is close to, but slightly worse than the 1-bit case. The choice of 1 or 2-bit samples is a trade-off between the slightly higher SNR and reduced sensitivity to gain and input power fluctuations of the 1-bit case and the reduced bandwidth, and hence wider delay beam, less sensitivity to delay errors, and ability to avoid RFI of the 2-bit case. For spectral line observations where there is likely to be excess recording capacity available since the sources only require limited bandwidth, it is advantageous to both sample with two bits and to oversample (sample faster than the Nyquist rate).

2. Fringe Rotation. VLBI systems do not adjust at the stations for the relative Dopper shifts of the signals due to earth rotation. This frequency shift, which can amount to tens of kHz, is accomplished in the correlator by multiplying by a tone. In 1-bit, XF correlators (all VLBI correlators except the VLBA) a three-level approximation of this tone is used. This causes a SNR loss of 0.96 when only one station is rotated as is typical. The VLBA correlator will use a many level approximation of the fringe rotation tone and these losses are almost entirely avoided.

3. Delay update. With digital data, it is not possible to cross correlate two bit streams with arbitrary delay offset. The delay has to be set in increments of one sample interval. This means there will be a variable delay error of up to $\pm 1/2$ sample interval. This causes a variable phase slope across the band which causes smearing of the data near one or both band edges, depending on where the phase is kept constant. If nothing is done about the effect, the phase at one band edge is kept constant and there is strong smearing at the other edge causing a SNR loss of 0.873. The NRAO Mark II correlator worked this way. If the phases are adjusted so that the phase of the center of the band is constant, there is smearing at both ends, but it is less severe and the SNR loss is 0.966. Finally, it is possible to eliminate the losses by rotating out the phase slope on data intervals short compared to the delay update interval. The VLBA correlator takes advantage of the fact that each station's data is in spectral form prior to cross correlation and applies a phase slope before cross correlation.

4. Local oscillator impurities. If any of the local oscillators used at a station to mix a signal from the sky frequency to baseband are not perfect sine waves, some power can be scattered to other frequencies and there will be a SNR loss. For the VLBA, such losses are thought to be less than about 2% (Bagri, private communication).

5. Non-square bandpasses. The baseband filters are typically not perfectly square and do not cut off completely above half the sampling frequency. The associated losses on the VLBA are thought to be less than a couple of percent. Non-square bandpasses, if they are not the same at all sites, can also lead to non-closing offsets which can make it difficult to obtain high dynamic range images.

6. Too few channels. If too few spectral channels are used, the separation of sidebands from the fringe rotation will not be perfect. Also there may be edge effects. This is most easily understood in the delay lag domain (the Fourier transform of the frequency spectrum). If there are two few lags, the signal, which rings to some extent, will have power outside of the sampled delay range. This signal is unmeasured and can lead to SNR loss. The VLBA correlator will probably be used mainly in modes where many channel spectra are generated and then averaged down to fewer channels. Sideband separation should be good in this case.

7. Polarization impurity. If the polarization response in each antenna is not perfect and not identical, there will be some SNR loss and the possibility of closure errors. On the VLBA, such losses should amount to less than about 4%.

8. Image rejection. The baseband converters have to separate the upper and lower sidebands. This process is done very well but not perfectly. Also, the unwanted sideband at the front end is rejected by filters and there is a small loss involved. On VLBA, these losses should be less than about 0.3%.

Other effects also can degrade performance from what is expected. Pointing errors cause amplitude loss. The troposphere, or moisture on the feeds and reflecting surfaces, can absorb some signal. The digitization and fringe rotation losses can be calculated accurately but many of the other effects depend on hardware details that can vary from site to site and time to time. In practice the total losses have to be determined empirically. They typically give an efficiency $\eta_s \sim 0.5$ for current XF correlators in the 1-bit Nyquist sampling mode. For the VLBA correlator, the losses should be somewhat less depending on processing mode.

In VLBI tradition there is a scaling factor known as the "b-factor". It is the factor by which the correlation coefficients delivered by the correlator must be multiplied to obtain the amplitude that would have been obtained by a perfect analog correlator using data from perfect electronics. For older correlators such as the NRAO spectral line correlator, this factor was about 2.5 and there was a tendency to confuse it with the SNR loss factor. Really it is just a scaling factor to account for imperfect normalization of the data. Some correlators, such as the Haystack design Mark III correlators (Haystack, Bonn, and Washington), adjust the data for all known effects so the b-factor is 1.0. Some such as the Caltech Block II used for Mark II, which has a b factor of about 13, leave some significant normalization step to the user. The VLBA correlator has many modes and the normalization factors vary between them. Eventually, this should all be hidden from the end users.

8.4.4 Image Sensitivity

If it is possible to make a VLBI image of a source using either self-calibration or using a nearby source as a phase reference, the noise limit in the image will be the combined sensitivity of the all baselines integrated over the full time of the observations. This is effectively the same as for a linked interferometer such as the VLA. This noise limit will determine the weakest features that can be seen in the absence of dynamic range limitations. The derivation of the image sensitivity, as for the baseline sensitivity, closely follows Walker (1989) .

Each cell in an image is a linear combination of each of the measured data points:

$$I(l,m) = C\sum_{n=1}^{2L} T_n W_n w_n \mathcal{V}_n e^{2\pi i(u_n l + v_n m)} . \tag{8.13}$$

$I(l,m)$ is the image point, $\mathcal{V}_n$ is the measured complex visibility data point located at (u_n, v_n), C is a normalization constant, T_n is the taper function, W_n is the weighting function, and w_n is the weight used to reflect the SNR of the data point. The sum is carried out over $2L$ points because, since the visibility function is Hermitian, the conjugate points to all measured points are also known. It is important to distinguish here between the weighting function W_n and the SNR weighting. The weighting function can either be unity ("natural weighting") or can reflect the local density in the (u,v) plane of other data points (the most common version being referred to as "uniform weighting"). The other form of weighting, by SNR, tends to get neglected in discussions of linked interferometers because all antennas are more-or-less equally sensitive. However it is often implemented in the software for such instruments as it is in AIPS. For VLBI there is a very wide range of sensitivities so the term can be very important.

To calculate the noise in the image, consider only the central point at $l = 0$ and $m = 0$. In the absence of strong features, the noise at this point is the same as elsewhere in the image and the math is simplified. At the central cell, the imaginary part of each data point does not contribute (cancelled by the

Hermitian conjugate point) and the intensity becomes

$$I(0,0) = 2C \sum_{n=1}^{L} T_n W_n w_n S_{Rn} \; . \tag{8.14}$$

To make the result come out in terms of flux density, C is set equal to

$$\frac{1}{2\sum_{n=1}^{L} T_n W_n w_n} \; .$$

The noise for this point is then given by

$$\Delta I = 2C \sqrt{\sum_{n=1}^{L} T_n^2 W_n^2 w_n^2 \Delta S_n^2} \; . \tag{8.15}$$

For the simplest case, i.e. no taper, natural weighting, and all points of equal SNR and ΔS_n, equation 8.15 reduces to $\Delta I = \Delta S/\sqrt{L}$ as expected for the standard deviation of the mean of L samples of a variable with standard deviation ΔS. If the ΔS_n are not equal, the best results with no taper and natural weighting are obtained with $w_n \propto 1/\Delta S_n^2$.

The lowest noise per pixel can be obtained with natural weighting and no taper. However, it is often desirable to use other imaging parameters. If the source is resolved, the longest baselines have little or no correlated flux density so using them in the imaging process only adds their noise but no information about the signal. Therefore, application of a taper such that only those baselines with signal contribute can enhance the detectability of the source. Effectively the resolution is lowered until the source is concentrated into a small number of resolution elements, raising the flux density per resolution element faster than the noise. The prices paid are higher noise per pixel and lower resolution. If too strong a taper is applied, data points with good signal are excluded from the image and the sensitivity is reduced. Weighting functions other than natural weighting are used to affect the quality of the beam. With natural weighting, most of the data tends to be concentrated toward the center of the (u, v) plane and the resolution is much less than that of the longest baselines. Uniform weighting can be used to reduce the emphasis on short baselines and to give higher resolution. Uniform weighting also has the effect of smoothing out uneven distributions of points and giving a better beam. The price paid for uniform weighting is a non-optimal weighting of the data points so the sensitivity is reduced. The actual magnitudes of the effects discussed here depend on the details of the sensitivities of the participating antennas and on the distribution of points in the (u, v) plane. For an extensive and illuminating discussion of weighting, see Briggs (1995).

The sensitivity of a VLBI observation cannot quite reach the level suggested by the above analysis because of effects of the fringe fitting and self-calibration needed to make images. There will be errors in the determination of the antenna calibration parameters that will introduce errors in the data above those set by noise. For the special case of a relatively strong, nearly unresolved source and N identical antennas, Cornwell (1981) showed that the sensitivity in an image is worse by a factor of $\sqrt{(N-1)/(N-3)}$ when self-calibration is used than when it is not needed. For more complicated cases, the corresponding analysis cannot be done, but experience indicates that the sensitivity is rarely reduced by a factor of 2 or 3 (Cornwell and Fomalont 1989).

In the presence of self-calibration, the measured scatter in off-source points in an image is not necessarily a good indicator of the sensitivity of the observation, although the deviation should be well under a factor of 2. In fact, the scatter, along with the measured flux density of any features not included in the self-calibration model, may decrease after self-calibration (Wieringa 1992). This is the result of the self-calibration forcing some of the deviations of the data from the model, whether from noise or unmodeled source structure, into the antenna gains. Also the dirty beam may have characteristics significantly different from the gaussian restoring beam often used after deconvolution (e.g., CLEAN), so the measured scatter may depend on details of the deconvolution (such as the number of CLEAN components).

8.5 Image Quality and Dynamic Range

The quality of an image produced by VLBI, or any other interferometer, is often determined by factors other than the sensitivity. If there are features in the image with significant flux density, the off source noise level will often be set by the limited dynamic range that can be obtained. Somewhat independently, the accuracy with which regions of emission are represented can also be limited by uniqueness concerns.

Limited dynamic range is usually the result of imperfections in the data such as closure errors. Self-calibration, upon which all modern images of very high dynamic range depend, is based on the assumption that all "calibration" offsets in the data are antenna based. For a variety of reasons, mostly having to do with imperfections in the hardware, this assumption will break down at some level. Such errors are a problem because they tend to be constant with time on each baseline. Therefore their effects are only reduced by the square root of the number of baselines (about the number of antennas) rather than the number of data points as with noise. At the VLA, such errors are a bit less than 1% for the continuum system and limit the dynamic range (ratio of image peak to off source rms) to about 10,000 to 20,000, unless special measures are taken to correct them. They are far more damaging than a few bad data points. Past VLBI network images have been limited to dynamic ranges of a few thousand while MERLIN, with only six antennas, has been able to reach tens of thousands. It is likely that network observations suffer from significant closure problems that are difficult to calibrate. For the VLBA, there has been an attempt to limit closure errors to

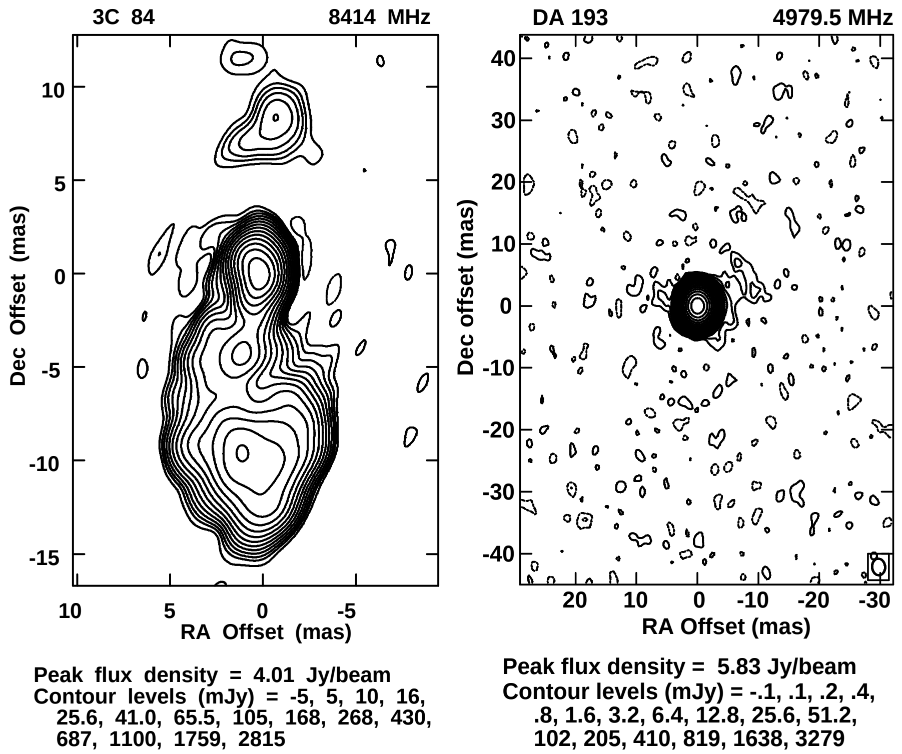

Figure 8.5: Two images made with VLBA data, and processed on the VLBA correlator, that show the capabilities of the instrument. (*a*) Image of 3C 84 from the VLBA correlator "First Science" observations made in August 1993. (*b*) Image of DA 193 from a November 1994 dynamic range test. The ratio of image peak to off-source rms is about 112,000 and is noise limited.

about 0.1%, and an test in which a dynamic range of 112,000 was obtained with no closure calibration suggests that this effort has been reasonably successful.

For phase referencing observations, the dynamic range may be limited by the quality of the phase calibration which is affected by fluctuations in the atmosphere. This would not be true for very weak sources for which the dynamic range is limited by noise. It would also not be true for sources strong enough to apply self-calibration. However there can be an intermediate range where phase calibration errors limit the dynamic range (see chapter 17).

Uniqueness is another problem which is somewhat different from dynamic range. It is the result of incomplete (u, v) plane coverage. It is seen easily when studies are made of the imaging ability of various array configurations using fake data based on a source of known structure. When images made from such data are subtracted from the input image, the errors are strongly concentrated in the region where there is emission. It is clear that the off source noise level is

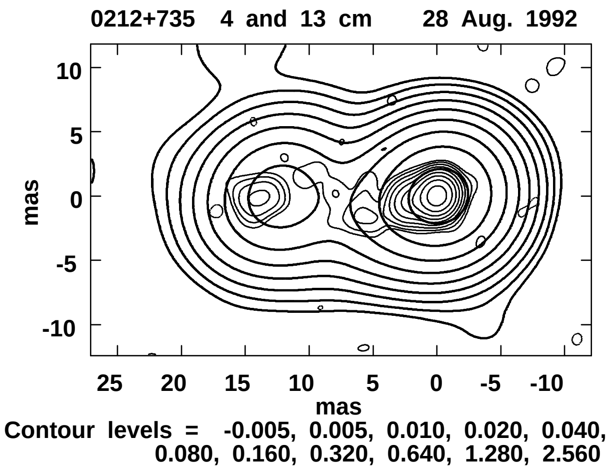

Figure 8.6: Images of 0212+735 at 4 cm (thin contours) and 13 cm contours made using data from a VLBA geodesy experiment. These images demonstrate a snapshot capability of the VLBA.

not a good indication of errors in the relative strength of regions with emission. This is simply an effect of the inability of the imaging algorithms to interpolate perfectly in the (u, v) plane. The presence of the effect is one of the reasons why dense (u, v) plane coverage and absence of large holes is so desirable.

8.5.1 Sample VLBA Images

Figure 8.5 shows two examples of images produced from long (u, v) tracks taken as VLBA test data. The first is of a complicated source, 3C 84, and reveals the presence a counterjet which analysis shows may provide a powerful probe of the material near a galactic nucleus (Walker, Romney and Benson 1994). This image was the first scientifically interesting image made with VLBA correlator data. The image quality is equivalent to anything made previously, despite being based on data from only 8 antennas and despite not having had some amplitude corrections for delay offsets done correctly. The second image is the highest dynamic range image yet produced with VLBI by a very large margin. It is of the slightly-resolved source, DA193, and has a dynamic range (peak to rms) of 112,000. This image demonstrates clearly that the VLBA can produce far higher dynamic range images than have ever been made with VLBI data before. It is also encouraging that the very first VLBA continuum image made using only VLBA hardware (3C 84) produced an important scientific result that reached publication less than a year after the observations were made.

The VLBA also has a snapshot capability that is quite useful. With far fewer baselines than the VLA (45 vs. 351), that snapshot capability certainly does not match that of the VLA, but the difference can be made up to a considerable degree by using a few, rather than only one, scan on each source. Figure 8.6 shows 4 cm (thin contours) and 13 cm (thick contours) images of one of the sources in a Mark III geodesy observation using 7 VLBA antennas (6 at 13 cm). The source was observed for about one minute about once per hour using 16 MHz bandwidth at 4 cm and 12 MHz bandwidth at 13 cm. The images are noise limited and both have peak/off-source dynamic ranges of over 1000. The 13 cm image is the example that will be used in practical VLBI imaging lecture in this volume. Thirty sources were observed in this 24-hr experiment and presumably could be imaged at a similar level (except those at very low declination for which the (u, v) coverage just is not as good). Even this experiment had fewer antennas than the full VLBA and had a quarter of the final bandwidth at each frequency. For observations on the full VLBA using the nominal bit rate at one band, and not spending a major fraction of the time slewing as do geodetic experiments, it should be possible to image roughly 100 sources at a dynamic range of about 1000 in a day or a larger number of sources at lower dynamic range in the same amount of time.

References

Briggs, D. S. 1995. *High Fidelity Deconvolution of Moderately Resolved Sources.* Ph. D. thesis, New Mexico Institute of Mining and Technology.

Cornwell, T. J. 1981. "An error analysis of calibration". VLA Scientific Memorandum 135, National Radio Astronomy Observatory.

Cornwell, T. J., & Fomalont, E. 1989. "Self-calibration". See Perley, Schwab and Bridle (1989), p. 185.

Crane, P. C., & Napier, P. J. 1989. "Sensitivity". See Perley, Schwab and Bridle (1989), p. 139.

Davenport, W. B., & Root, R. L. 1958. *An Introduction to the Theory of Random Signals and Noise.* New York: McGraw-Hill.

Perley, R. A., Schwab, F. R., & Bridle, A. H. (Eds.) 1989. *Synthesis Imaging in Radio Astronomy.* San Francisco: Astronomical Society of the Pacific.

Readhead, A. C. S., & Wilkinson, P. N. 1978. "The mapping of compact radio sources from VLBI data". *Astrophys. J.* **223**, 25.

Thomasson, P. 1986. "MERLIN". *Quart. J. Roy. Astron. Soc.* **27**, 413.

Thompson, A. R., Moran, J. M., & Swenson, G. W., Jr. 1986. *Interferometry and Synthesis in Radio Astronomy.* New York: Wiley-Interscience. First (1991) and second (1994) reprintings by Krieger Pub. Co., Malabar (Florida).

Walker, R. C. 1989. "Sensitivity". In M. Felli and R. Spencer (Eds.), *Very Long Baseline Interferometry.* Volume 283 of *NATO ASI Series C.* Dordrecht: Kluwer, p. 163.

Walker, R. C., Romney, J. D., & Benson, J. M. 1994. "Detection of a VLBI counterjet in NGC 1275: A possible probe of the parsec-scale accretion region". *Astrophys. J.* **430**, L45.

Wieringa, M. H. 1992. "An investigation of the telescope based calibration methods 'redundancy' and 'self-cal'". *Experim. Astron.* **2**, 203.

Wilkinson, P. N. 1991. "The MERLIN—Phase 2". In T. J. Cornwell and R. A. Perley (Eds.), *IAU Coll. 131, Radio Interferometry: Theory, Techniques, and Applications.* Volume 19 of *ASP Conference Series.* San Francisco: Astron. Soc. of the Pacific, p. 381.